

**UNCLASSIFIED**

---

---

**AD 296 232**

*Reproduced  
by the*

**ARMED SERVICES TECHNICAL INFORMATION AGENCY  
ARLINGTON HALL STATION  
ARLINGTON 12, VIRGINIA**



---

---

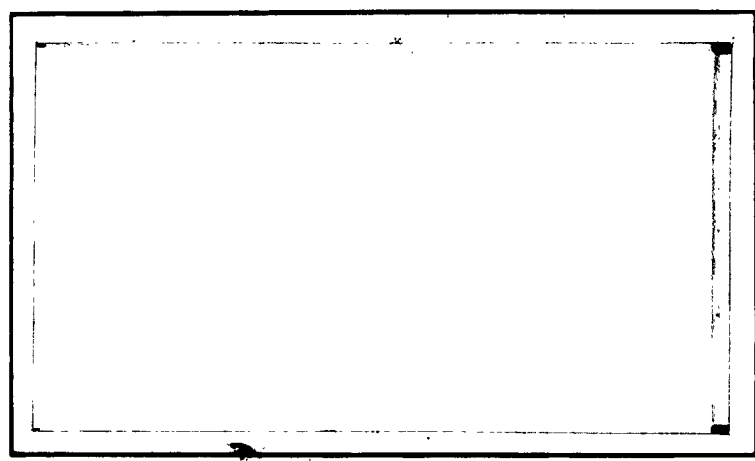
**UNCLASSIFIED**

NOTICE: When government or other drawings, specifications or other data are used for any purpose other than in connection with a definitely related government procurement operation, the U. S. Government thereby incurs no responsibility, nor any obligation whatsoever; and the fact that the Government may have formulated, furnished, or in any way supplied the said drawings, specifications, or other data is not to be regarded by implication or otherwise as in any manner licensing the holder or any other person or corporation, or conveying any rights or permission to manufacture, use or sell any patented invention that may in any way be related thereto.

63-2-4

296232

CATALOGED BY ASTIA  
AS AD No. \_\_\_\_\_



296 232

ASTIA  
RECEIVED  
FEB 13 1963  
TISIA

**REPUBLIC**  
AVIATION CORPORATION

OFFICE OF NAVAL RESEARCH  
Contract Nonr-3285(00)  
Task No. NR 099-350

Final Technical Report

MAGNETIC FIELD EFFECTS  
IN THERMIONIC PLASMA DIODES

by

Alfred Schock  
William E. Eaton  
Charles L. Eisen  
Bernard Wolk

Power Conversion Systems Division  
Republic Aviation Corporation  
Farmingdale, L.I., New York

January 1963

Reproduction in whole or in part is permitted for  
any purpose of the United States Government

## FOREWORD

This is the final report on an investigation into the effects of magnetic fields on thermionic diodes, which was sponsored by the Office of Naval Research under Contract Nonr-3285(00).

Since the theoretical analyses undertaken as part of this program have been adequately covered in previous publications, only a brief summary of their results is included. The present report is primarily confined to the experimental program. To maintain a reasonable length, only those measurements required to illustrate the conclusions are presented.

The work was directed by Alfred Schock, under the technical supervision of CDR John J. Connelly of the ONR Power Branch.

ABSTRACT

Experiments to determine the effect of transverse and longitudinal magnetic fields on thermionic current transmission are described. The results obtained are in qualitative agreement with theoretical predictions, and suggest the possibility of using magnetic modulation for a. c. generation.

## CONTENTS

<u>Section</u>	<u>Title</u>	<u>Page</u>
	Foreword	ii
	Abstract	iii
I	Introduction	1
II	Conclusions	3
III	Experimental Apparatus	4
IV	Test Procedure	9
V	Results and Discussion	13
VI	References	21
	Appendix A - Master Distribution List	A-1

## LIST OF ILLUSTRATIONS

<u>Figure</u>	<u>Title</u>	<u>Page</u>
1	Planar Diode Test Setup, to Vary Magnetic Field Orientation	6
2	Cylindrical Diode	7
3	Planar Diode	8
4	Test Circuit Diagram	12
5	Theoretical Effect of Diode Voltage $V$ and Transverse Magnetic Field $B_{\perp}$ on Current Transmission	22
6	Transverse Field Effect in Low Pressure Diode	23
7	Effect of Transverse Fields on Oscillations	23
8	Transverse Field Effects on Current-Voltage Characteristics at Various Cesium Pressures	24
9	Ignited Diode Operation in Presence of Transverse Magnetic Fields	25
10	Effect of Transverse Fields on Ignition Voltage	25
11	Transverse Field Effects on Power-Voltage Characteristics at Various Cesium Pressures	26
12	Effect of Transverse Fields on Maximum Power Output, at Various Cesium Pressures	27
13	Comparison of Theoretical and Measured Magnetic Field Effects on Maximum Power Output	28
14	Theoretical Fraction of Electrons Reaching Collector Without Suffering Collisions	29
15	Effect of Strong Magnetic Field at Various Orientations	30
16	Effect of Various Longitudinal Fields with Constant Transverse Fields	30
17	Effect of Sinusoidal Magnetic Fields on Oscillatory Diode	31
18	Effect of Sinusoidal Magnetic Fields on Thermionic Diodes at Various Cesium Pressures	32
19	Circuit for Demonstrating A. C. Generation	33
20	Typical Results of A. C. Demonstration	34

## SECTION I - INTRODUCTION

The effects of magnetic fields on current transmission in thermionic energy converters are of interest for three reasons: the possible deleterious effect of self-induced magnetic fields; the potential usefulness of applied magnetic fields for current modulation and a. c. generation; and their possible aid in understanding the oscillatory and ignited modes of operation.

A previous analysis<sup>1</sup> had shown that under certain conditions the self-induced, transverse magnetic fields present in large thermionic converters could materially reduce the fraction of emitted electrons reaching the collector; but that this effect could, in principle,<sup>2</sup> be counteracted by the application of a longitudinal magnetic field.

A subsequent study examined the possibility of using magnetic modulation for thermionic a. c. generation, a subject of some importance in view of the low voltage, high current output of d. c. thermionic diodes. In principle, the application of an appropriate magnetic modulating field can produce a periodically varying diode current, the a. c. component of which could be extracted (and stepped up) by means of a transformer.

Such a scheme necessarily entails some loss of efficiency. To assess the magnitude of that loss, both a d. c. analysis<sup>3</sup> and a corresponding a. c. analysis<sup>4</sup> were carried out. Comparison of the results indicates that for a given collector work function and emitter temperature, the a. c. generation scheme selected has a maximum efficiency equal to approximately 70% of the corresponding d. c. efficiency.

Since the theoretical predictions of magnetic field effects were based on a microscopic model which assumed that each electron is unaffected by all other particles present, their strict validity is limited to thermionic diodes whose cesium density is high enough for complete space charge cancellation, but low enough to permit collisions to be neglected (e. g.,  $T_{Cs} = 100^\circ C$ ). For the case of high

density thermionic diodes, i. e., those in which the electrode spacing greatly exceeds the electrons' mean free path, the interaction of the magnetic fields with the plasma would have to be analyzed from a macroscopic (MHD) point of view.

Since such an analysis would in any case yield no information about the important case of intermediate cesium densities, experimental measurements are required to cover the entire range of interest. The only reported<sup>5</sup> measurements on these effects are somewhat fragmentary, and are confined to the range of relatively weak magnetic fields ( $B < 80$  gauss). The present paper describes a far more extensive investigation of the subject, aimed at verifying the theoretical predictions at low cesium pressures, and determining the extent of their validity at higher plasma densities and under "ignited" operation.

## SECTION II - CONCLUSIONS

1. The effect of transverse magnetic fields on thermionic current transmission is in qualitative agreement with theoretical predictions.
2. As expected, the magnetic field effects diminish at high cesium densities.
3. In thermionic converters composed of small diodes, at high cesium pressures and close electrode spacings, self-induced magnetic field effects can be reduced to a negligible role by proper design.
4. Under different operating conditions (large diodes, moderate cesium pressures), self-induced fields can result in serious performance degradation.
5. As predicted by theory, the adverse effect of transverse magnetic fields can be virtually eliminated by applying a suitable longitudinal field.
6. Even at higher cesium pressures, applied magnetic fields of practicable magnitude can produce substantial current modulation.
7. The results suggest the feasibility of employing magnetic modulation for thermionic a. c. generation.

### SECTION III - EXPERIMENTAL APPARATUS

Most of the experiments employed a cylindrical diode surrounded by a coaxial solenoidal field coil, which produced an axial magnetic field transverse to the radial diode current. In addition, a number of experiments used a planar diode located in the gap of an iron core electromagnet, as shown in Figure 1. By varying the magnet's field strength and the orientation of its pole faces with respect to the diode, any combination of longitudinal and transverse fields could be simulated.

The cylindrical and planar diodes had emitter areas of 13 and 3.75 cm<sup>2</sup>, and electrode spacings of 40 and 42 mil, respectively. In general, it was desired to make the diodes large enough to minimize end effects, yet compact enough to fit within their respective magnets. Nonmagnetic materials were used throughout the diode and its support structure.

Both types of diodes utilized emitters of porous tungsten impregnated with thorium. This choice of an intermediate work function material was dictated by the desire to test the same device over the entire range of cesium pressures, in both the ignited and extinguished modes of operation.

As shown by Figure 2, the cylindrical diode's emitter was in the form of an annular sleeve (50-mil thick) supported by a tantalum cup (20-mil wall). This support cup also acted as an electrical lead, and as a seal between the heater and the cesium. A similar support cup was used in the planar diode, with the disk-shaped emitter held against the cup's end face by means of a threaded tantalum retaining ring (Figure 3). To minimize stray currents, the outer face of the retaining ring was coated with alumina insulator, and side shields were inserted between the emitter support cup and the collector. These shields were made of 1-mil tantalum foil, and were electrically isolated from both emitter and collector.

Initially, it was decided not to resort to electron bombardment for heating the emitter, because of the perturbation of the bombardment current by the magnetic field. However, since alternate heating methods (radiation, conduction) proved unsatisfactory at the higher emitter temperatures, the use of electron bombardment could not be avoided. As explained in the section on test procedure, satisfactory methods for eliminating the effect of the above perturbation were devised.

Both molybdenum and stainless steel (type 304) collectors were tested, and resulted in substantially the same diode performance. In each case, the collector formed part of the diode envelope, and was in thermal contact with a cooling coil. Depending on the desired collector temperature, either water or air was used as coolant.

To minimize the danger of contaminating the diode, it was desired to avoid the use of brazing alloys and of (active) bonding materials for joining ceramics to metals. Moreover, to facilitate maintenance, it was decided to design the diode so that either side (vacuum or cesium) could be opened without affecting the other. To achieve these ends, both sides were closed by means of knife edge seals, compressed by stainless steel bolts with appropriate high temperature characteristics. Besides the metallic knife edges, the cesium side seal employed an additional ceramic double knife edge to provide electrical insulation between emitter and collector. The ceramic knife edges were made from high purity, high density alumina rings, and diamond ground to a 60° bevel, with a 5 mil flat at the edges which contact the copper gaskets. The gaskets were flanged to assure proper alignment and were annealed after machining. After some initial difficulties in arriving at the proper choice of materials, the seals described above proved highly reliable, and provided valuable flexibility for servicing the diode.

The electron source consisted of a directly heated tungsten filament and the emitted electrons were accelerated into the emitter support cup by means of a high voltage d. c. power supply.

In addition to copper tubing pumpdown legs for the vacuum and cesium sections, each diode was provided with a cesium reservoir. After some early difficulties caused by reaction between copper and liquid cesium, subsequent cesium reservoirs were made of stainless steel.

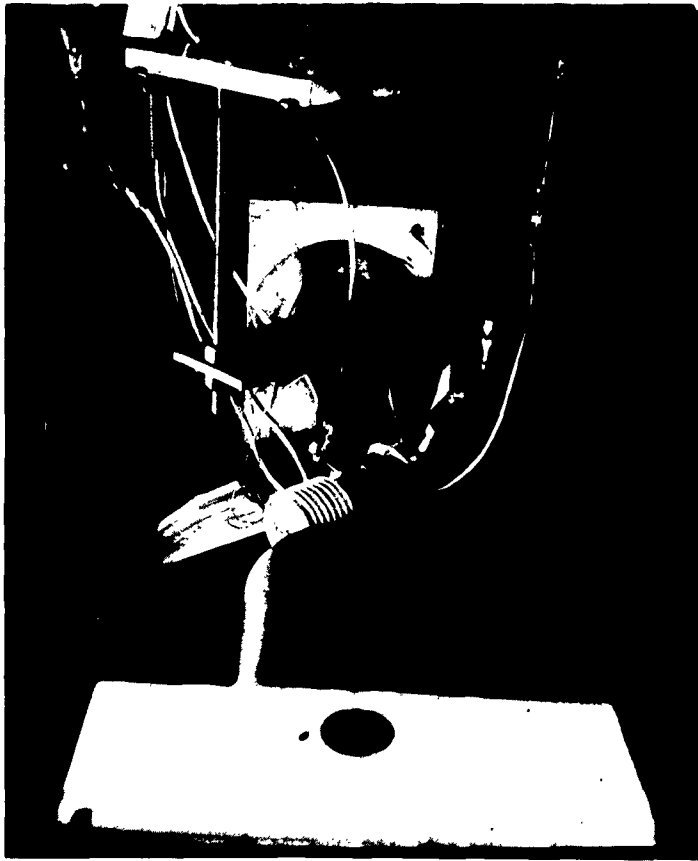


**Figure 1. Planar Diode Test Setup, to Vary Magnetic Field Orientation**

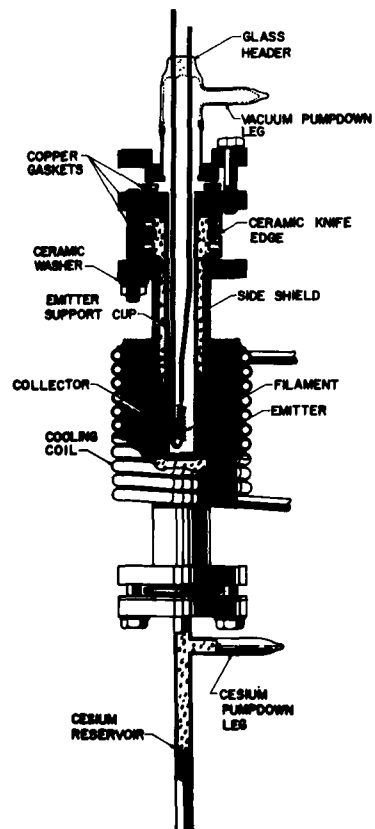


Figure 2. Cylindrical Diode

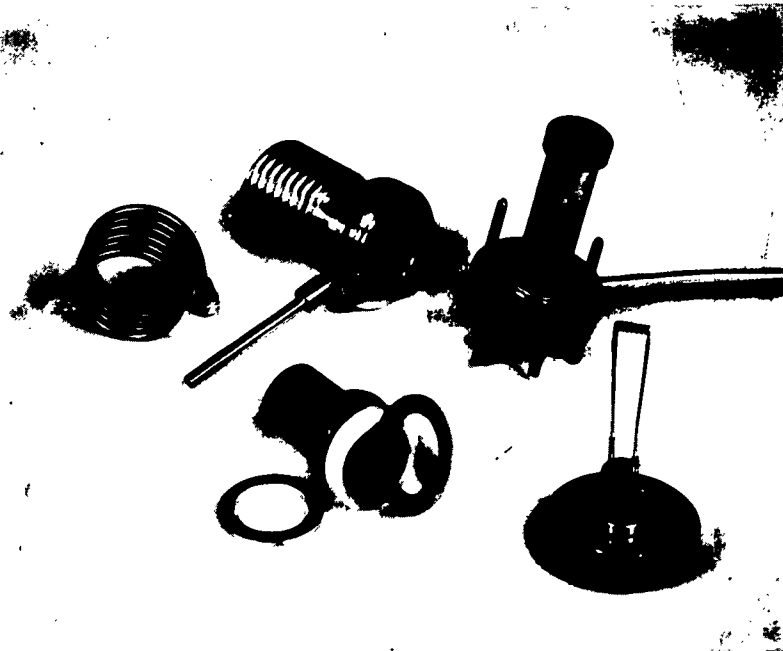
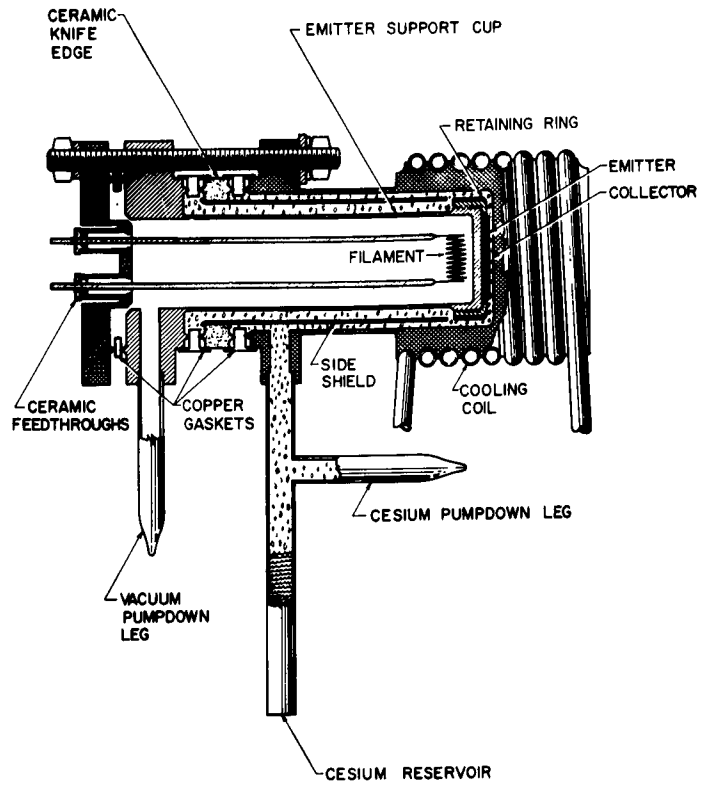


Figure 3. Planar Diode

#### SECTION IV - TEST PROCEDURE

The primary object of the experiments was to measure diode current as a function of voltage and magnetic field strength, for various values of emitter temperature and cesium reservoir temperature.

After assembly and pumpdown, each diode was outgassed with its envelope at 400°C, followed by heating the emitter to its normal operating temperature. Separate pumping systems were used for the two sections, and outgassing continued until both pressures were below  $10^{-6}$  mm Hg. After pinch-off, the cesium (99.9% purity) was released by crushing the glass ampule which had been introduced into the copper tube attached to the pumpdown leg. After transferring the cesium to its permanent (stainless steel) reservoir by distillation, the temporary copper section containing the crushed glass was removed by pinch-off.

During testing, each diode was mounted in its magnet, and its reservoir and envelope temperatures were controlled by an electrically heated air stream. All temperatures (except that of the emitter) were monitored by thermocouples. Although no provisions were made for pyrometry during testing, the emitter temperature could be estimated from a previous calibration against power input. This calibration was obtained in a vacuum diode, identical with the cesium diode except for a sapphire window to permit pyrometric observation.

In spite of the high accelerating voltage between the tungsten filament and the emitter ( $> 1000$  v), transverse magnetic fields were found to produce substantial reductions in bombardment current. The resultant drop in emitter temperature eventually caused a reduction in diode current. This secondary effect was separate from the direct influence of magnetic fields on current transmission.

One method of measuring the direct magnetic field effect at constant emitter temperature was to readjust the heater power supply after the imposition of the magnetic field, so as to maintain the same heat input power. In this case, the diode current was measured after a new equilibrium had been established.

An alternate method for avoiding the secondary effect of the magnetic field was to take measurements immediately ( $< 1$  sec) after closing the diode circuit and applying the magnetic field. This method, which was generally preferred because of its speed and simplicity, depended on the heat capacity of the emitter structure to maintain an essentially constant temperature during the measurement. It had the additional advantage of avoiding temperature perturbation due to electron cooling, and gave highly reproducible results.

At any given emitter temperature, reservoir temperature, and magnetic field strength, the relationship between diode current and voltage was measured by feeding the respective signals to an xy-oscilloscope (Tektronix, Model 536) and recording the data photographically. Both static and dynamic measurements were made: the former under steady load conditions; the latter with diode voltage varied at the rate of 60 cps. The two methods gave good agreement, and the dynamic method was generally preferred because of its speed and convenience.

The external circuit used for the dynamic measurements is shown in Figure 4. Alternating current (110 v, 60 cps) was passed through a variable autotransformer to a stepdown transformer, whose secondary winding was in series with the test diode. A bank of 12-volt batteries and a potentiometer provided means for applying an adjustable bias. By varying the autotransformer and potentiometer, the upper and lower limits of the voltage sweep could be varied at will. In addition to the above components, the circuit contained a small load resistance for measuring the diode current, a set of relays for simultaneously closing the diode circuit and activating the magnet, and a selector switch to bypass the a. c. signal when static measurements were desired.

After reaching the desired emitter and cesium reservoir temperatures, sufficient time was allowed for the cesium distribution to reach an equilibrium. The measurements were taken in the form of current-voltage characteristics at

various magnetic field strengths. To facilitate comparison and interpretation, all the curves for a given set of emitter and reservoir temperatures were superimposed on the same photograph. After each trace was recorded, sufficient time was allowed to reestablish thermal equilibrium.

Under certain conditions of cesium pressure and emitter temperature, the I-V characteristic was found to be double-branched, corresponding to the extinguished and ignited modes of operation. Except where otherwise noted, the lower (extinguished) branch of the I-V trace was electronically blanked out for the sake of clarity, and only the upper (ignited) branch was recorded.

In addition to the above I-V measurements, it was also desired to obtain curves of diode power  $P$  versus voltage, under dynamic test conditions (60 cps). To do this, the current and voltage signals were fed to an electronic analog multiplier, whose output  $P$  was displayed on an xy-oscilloscope. Inspection of the resultant P-V traces yielded the maximum power for each field strength.

In a similar manner, the output power could be displayed as a function of field strength rather than voltage. For a constant magnetic field and a 60-cps voltage sweep, this resulted in a vertical line whose peak denoted the maximum power for that field strength. By manually varying the magnetic field, a picture of  $P_{\max}$  versus  $B_{\perp}$  was obtained. To facilitate comparison with theory, scaling was adjusted so as to display the ratio of  $P_{\max}$  to its value when  $B = 0$  (at the same emitter temperature and cesium pressure).

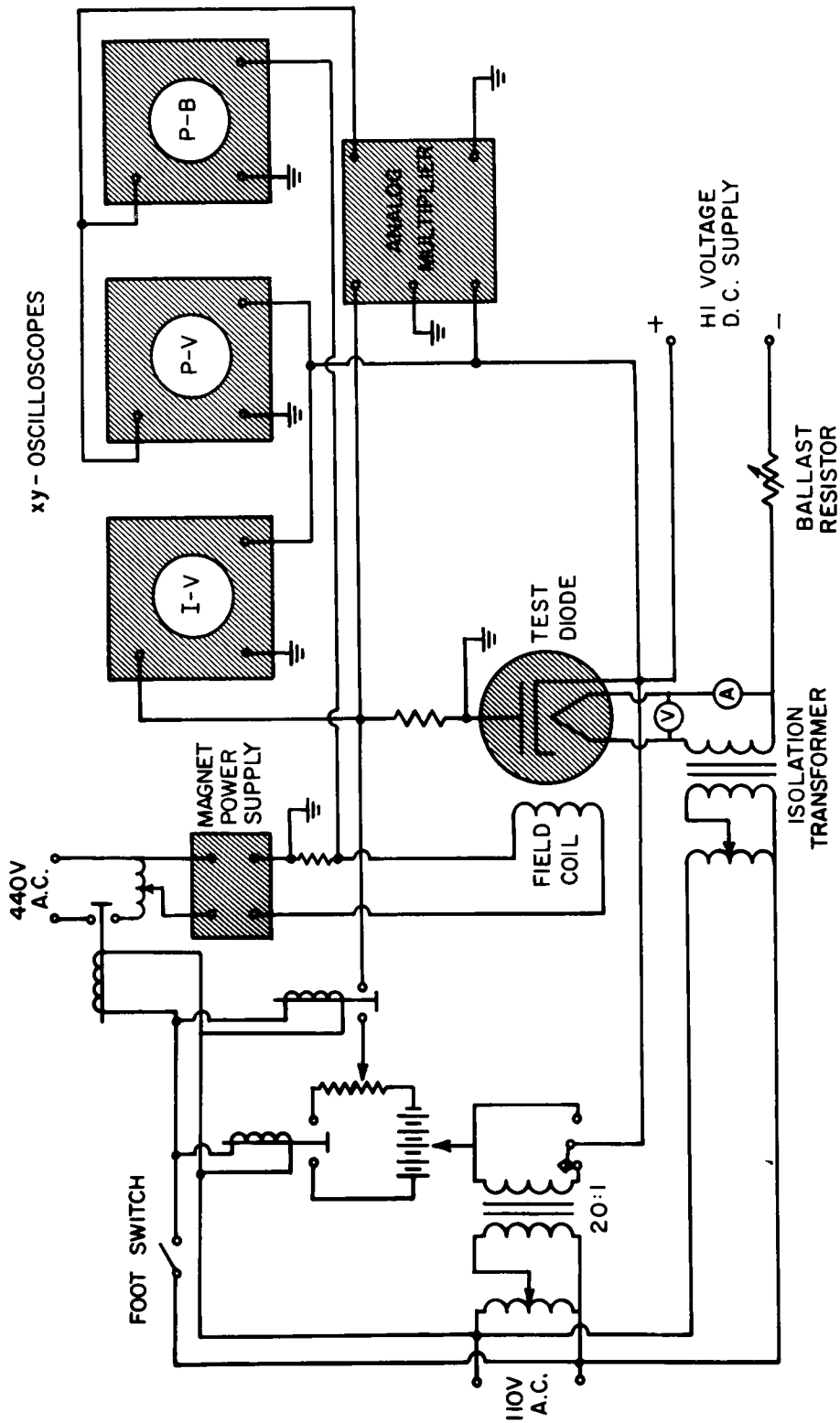


Figure 4. Test Circuit Diagram

## SECTION V - RESULTS AND DISCUSSION

Before presenting the experimental measurements, let us briefly review the results of the theoretical (collisionless) analysis. It was shown<sup>1</sup> that when a diode of emitter work function  $\phi_E$  and temperature  $T_E$ , electrode spacing  $D$ , and collector work function  $\phi_C$  is subjected to a load voltage  $V$  and transverse magnetic field  $B_{\perp}$ , the fraction of emitted electrons reaching the collector is given by

$$f = \frac{1}{2} \operatorname{erfc} [\mathcal{B} - (v/4\mathcal{B})] + \frac{1}{2} \operatorname{erfc} [\mathcal{B} + (v/4\mathcal{B})] \exp \mathcal{U}, \quad (1)$$

where  $\mathcal{B} \equiv (8m\kappa T_E)^{-\frac{1}{2}} eDB_{\perp}$ ,

$$\mathcal{U} \equiv (e/\kappa T_E) (\phi_E - \phi_C - V),$$

and where  $e$  and  $m$  denote the charge and mass of an electron, and  $\kappa$  is Boltzmann's constant. The above equation is illustrated by Figure 5, which predicts that the diode current is most sensitive to magnetic fields when the load voltage equals the difference between the emitter and collector work functions ( $v = 0$ ).

Typical experimental results for a low pressure diode are illustrated by Figure 6. Comparison with Figure 5 shows good qualitative agreement between theory and experiment at low cesium densities. However, two points of difference should be noted:

The first relates to the diode characteristics for the case when  $B = 0$ . As shown by Figure 5, Eq. (1) predicts the usual idealized curve for complete space charge cancellation and no internal resistance. For the actual diode illustrated by Figure 6, however, the characteristic to the left of the "knee" is not flat, because of the occurrence of high frequency oscillations. Incidentally, Figure 6 illustrates that these oscillations can frequently be suppressed by applying a magnetic field. In fact, under certain conditions a very weak transverse

magnetic field can actually increase the diode current by eliminating these oscillations, as shown by Figure 7.

The second noteworthy point of difference between theory and experiment relates to diode characteristics at low (or negative) load voltages. Contrary to theoretical predictions, the curves do not rise to the level of the saturation current, but tend to flatten out at lower levels.

The transverse field effect measurements over the entire range of cesium pressures are summarized by Figure 8, which may be viewed as a four-dimensional representation of  $I$  versus  $V$ ,  $B_{\perp}$ , and  $T_{Cs}$ . Only that portion of the I-V characteristic which lies in the power producing quadrant is shown. The data shown are for two representative emitter temperatures. Similar results were obtained at other temperatures.

Parenthetically, it should be noted that transverse magnetic fields can have a pronounced influence on the ignited mode of operation. These effects are best seen by unblanking the lower (extinguished) branch of the I-V trace. For example, in the case illustrated by Figure 9 the cesium pressure is high enough ( $T_{Cs} = 250^{\circ}\text{C}$ ) so that reduction of the load resistance produces a smooth transition into the ignited region, without any discontinuous jump in current. This is shown by the  $B_{\perp} = 0$  trace, and is seen to be still true at  $B_{\perp} = 250$  gauss. Increasing the transverse field to 500 gauss, however, changes the I-V characteristic from a single-branched to a double-branched curve, the upper and lower branches corresponding respectively to the ignited and extinguished modes of operation. Thus, at  $B_{\perp} = 500$  gauss, the load voltage must be reduced to approximately zero before ignition commences. In general, increasing the transverse field decreases the ignition voltage, as is graphically depicted by Figure 10.

Comparison of Figures 5 and 8 shows that at increasing cesium pressures the current transmission becomes progressively less sensitive to the magnetic field. However, it is seen that at all but the very highest cesium pressure, magnetic fields can exert a pronounced effect on current transmission.

Corresponding measurements of output power versus load voltage at various field strengths and cesium pressures are displayed in Figure 11. Each curve passes through  $P = 0$  twice: at short-circuit ( $V = 0$ ), and at open circuit ( $I = 0$ ). The optimum load voltage, i. e. the voltage which maximizes the power, can be determined by inspection of the P-V curves. As expected,  $V_{\text{opt}}$  decreases at increasing cesium pressure, and also at increasing field strengths.

Under certain conditions (e. g.,  $T_{\text{Cs}} = 200^\circ\text{C}$ , Figure 8) the I-V curves may consist of two convex segments, meeting at the point of transition from the ignited to the extinguished mode. Under this condition, the P-V curve can exhibit more than one peak, as shown by Figure 11.

Finally, it is of interest to examine the effect of transverse fields on the maximum output power (i. e., with optimized load voltage). Figure 12 presents a series of P-B traces for various cesium pressures. The discrete, vertical lines arise because the load voltage is swept at 60 cps, while the magnetic field is manually varied at a slower rate. The peak of each line indicates the maximum power at that field strength. Since the vertical scale was adjusted to make the  $E = 0$  line extend over the full height of each picture, the envelope of the lines represents the effect of  $B_{\perp}$  on  $P_{\text{max}}/P_0$ , the ratio of the maximum power to its zero field value.

In addition to the data shown in Figure 12, a series of more detailed measurements were made, covering the entire range of magnetic field strengths under investigation. The results for the various cesium pressures are assembled in Figure 13, together with the theoretical curve of  $P_{\text{max}}/P_0$  versus  $B_{\perp}$ . The latter was computed from the relation

$$\frac{P}{P_0} = \frac{f V}{\phi_E - \phi_A}, \quad (2)$$

with the transmission fraction  $f$  given by Eq. (1). The computation assumed that  $\phi_E = 3.2$  v,  $\phi_A = 1.6$  v, and  $D = 1$  mm.

Figure 13 illustrates the qualitative similarity between the theoretical and experimental curves, except at their lower ends. Although the field effect clearly diminishes at higher cesium pressures, it is seen that sufficiently

strong magnetic fields cause substantial reductions in power output, even in high pressure diodes. It is interesting to observe that all the experimental curves have approximately the same shape. Thus, as far as the magnetic field effect is concerned, increasing the cesium pressure is roughly equivalent to dividing the field strength by a constant factor. For example, to produce the same effect at the highest pressure ( $T_{Cs} = 350^\circ\text{C}$ ) as at the lowest ( $T_{Cs} = 100^\circ\text{C}$ ), the transverse field must be increased by a factor of  $\sim 50$ .

To help understand why, even at the lowest cesium pressures, the results are not in quantitative agreement with the collisionless theory, it is of interest to compute what fraction of the emitted electrons actually reaches the collector without suffering any collisions. Consider a cesium diode of electrode spacing  $D$  and mean free electron path  $\lambda$ , emitting electrons with a velocity distribution<sup>1</sup>

$$dJ = (2J_0/\pi) u^3 \exp(-u^2) \sin \theta \cos \theta \, d\theta \, du, \quad (3)$$

where

$$u \equiv (m/2kT_e)^{1/2} v,$$

and where  $\theta$  is the angle between the emission velocity  $\underline{v}$  and a normal to the emitter,  $\phi$  is the azimuthal angle, and  $J_0$  is the emitted current density. Since an electron emitted at an angle  $\theta$  must traverse a path length  $D/\cos \theta$  to reach the collector, the probability  $p$  of its arrival at the collector without having suffered a collision is

$$p = \exp(-D/\lambda \cos \theta). \quad (4)$$

Consequently, the uncollided arrival fraction  $f_u$  is given by

$$f_u = J/J_0 = (2/\pi) \int_0^\infty \int_0^{1/2\pi} \int_0^{2\pi} u^3 \exp(-u^2) \sin \theta \cos \theta \exp(-D/\lambda \cos \theta) \, d\phi \, d\theta \, du;$$

hence 
$$f_u = \left(1 - \frac{D}{\lambda}\right) \exp\left(-\frac{D}{\lambda}\right) - \left(\frac{D}{\lambda}\right)^2 \text{Ei}\left(-\frac{D}{\lambda}\right), \quad (5)$$

where  $\text{Ei}(-x)$  denotes the exponential integral  $-\int_x^\infty t^{-1} e^{-t} \, dt$ . Equation (5) is illustrated by Figure 14. It should be noted that with an electrode spacing of one mean free path (e.g.,  $D = 1 \text{ mm}$ ,  $T_{Cs} \approx 160^\circ\text{C}$ ), less than 22% of the emitted

electrons reach the collector without suffering collisions. For a spacing of two mean free paths ( $T_{\text{Cs}} \approx 180^\circ\text{C}$ ) the uncollided fraction drops to 6%. Even at the lowest cesium density adequate for space charge neutralization ( $T_{\text{Cs}} \approx 100^\circ\text{C}$ ,  $\lambda \approx 2$  cm,  $\lambda/D = 0.05$ ) almost 10% of the electrons suffer collisions before arriving at the collector.

In view of the above conclusions, exact agreement between theoretical predictions and experimental results would not be expected. In fact, the qualitative agreement existing even at moderately high cesium pressures and under ignited operation is surprisingly good, considering that the average electron must experience numerous collisions under these conditions.

The transverse field effect measurements reported above indicate that thermionic converters operating at high cesium pressures and close spacings would be virtually unaffected by self-induced magnetic fields, except at very high field strengths. Such strong fields can, however, be avoided by building a converter consisting of many small diodes, and arranging these so as to prevent the buildup of additive magnetic fields. Proper design can ensure that each diode sees only the effect of its own field, without any contributions from neighboring cells.

The theoretical effect of a longitudinal magnetic field was examined in a subsequent analysis.<sup>2</sup> When a plasma diode is simultaneously subjected to a strong transverse field  $B_{\perp}$  and longitudinal field  $B_{\parallel}$ , collisionless analysis predicts a transmission fraction

$$f = B_{\parallel} / (B_{\perp}^2 + B_{\parallel}^2)^{1/2} = \sin \alpha, \quad (6)$$

where  $\alpha$  is the angle between the combined magnetic fields and the surface of the emitter. The above analysis assumed that  $V = \phi_{\text{e}} - \phi_{\text{c}}$ , and that the transverse field by itself is strong enough for virtually complete current suppression.

The measured effects of combined longitudinal and transverse fields are illustrated by Figures 15 and 16. The former shows the effect of a constant magnetic field at various orientations. As expected, reducing the angle  $\alpha$  between field and emitter reduces the current transmission. Although theory predicts full

transmission when the field is normal to the emitter, a slight current reduction was observed at  $\alpha = 90^\circ$ . This may be attributed either to the collisional effects discussed above, or to stray radial currents that may have been present in spite of the efforts to eliminate them. Such radial current components would, of course, be reduced by the axial field.

Finally, Figure 16 illustrates the effect on current transmission of increasing the longitudinal field  $B_{\parallel}$ , while maintaining a constant transverse field  $B_{\perp}$ . As predicted, the current-reducing effect of the  $B_{\perp}$  field is counteracted by the application of the  $B$  field. Thus, if a thermionic generator were operated under conditions where self-induced fields did play a harmful role, their effect could be mitigated by adding a suitable longitudinal field.

In addition to obtaining qualitative confirmation of the theoretical predictions, it was desired to demonstrate the feasibility of periodic current modulation by means of a magnetic modulating signal. To this end, a 60-cps alternating current of adjustable amplitude was passed directly through the solenoidal field coil surrounding the cylindrical diode. The resultant diode current ripple has twice the frequency of the modulating field, since the effect of the axial magnetic field is independent of the direction of that field.

Figure 17 depicts the influence of sinusoidal magnetic fields on a low pressure diode operating in the oscillatory mode. The resultant 120-cps signal superimposed on the 400-kc diode current suggests possible application in the field of communications. The effect of alternating fields on diodes operating at intermediate cesium pressures is shown by Figure 18. The magnitude of the load impedance ( $\sim 0.8$  ohm) used in each case can be estimated from the slope of the accompanying I-V curves. The fact that these are somewhat U-shaped, rather than straight load lines, is presumably due to inductive effects in the rheostat and test circuit. This also accounts for the slight asymmetry of the current versus time traces.

Unfortunately, the available equipment limited the maximum alternating magnetic field to the relatively low rms value of 215 gauss. Nevertheless, Figure 18 illustrates that a comparatively weak field can produce quite substantial current modulation, even at moderately high cesium pressures. Moreover, Figures 8 and 13 suggest the likelihood that high pressure diodes can also be modulated by applying sufficiently strong magnetic signals.

Finally, it was desired to demonstrate, at least in a crude fashion, the possibility of thermionic a. c. generation by means of magnetic modulation. To do so efficiently would have required additional apparatus, beyond the scope of the present work. However, it was possible to produce a qualitative demonstration by means of the simple circuit shown in Figure 19. The magnetic field coil was energized by a 60-cps alternating current plus a direct current of sufficient magnitude to keep the field from reversing direction. The modulated 60-cps diode current was then passed through a 40:1 step-up transformer, whose secondary winding was in series with a load resistance R and a capacitor C. The latter was added to improve the output wave shape.

The use of the superimposed a. c. and d. c. field current resulted in a modulated diode current without the sharp cusps exhibited in Figure 18. Moreover, it produced a maximum field strength equal to twice the value attainable without the d. c. supply. This stronger field made it possible to demonstrate thermionic a. c. generation even in a high pressure diode ( $T_{Cs} = 307^{\circ}C$ ).

Typical results achieved with the above circuit are illustrated in Figure 20, which shows the time variation of field current, diode current and voltage, secondary voltage and load voltage. In each case, the line voltage was used for triggering the oscilloscope, to show the phase relationship of the various signals. The observed phase shifts, which presumably result from the reactance of the transformer, are illustrated even better by the accompanying I-V traces.

It should be emphasized that the various circuit parameters were rather arbitrarily chosen to optimize the output wave shape; they do not represent a maximization of load power or efficiency. The last column of Figure 20 shows

a peak to peak load voltage of 20 v, and a peak power of 0.57 watt. Note, however, that the load voltage was not truly sinusoidal, because of the non-linearity of the magnetic field effect. To generate a sinusoidal output would require a specially tailored magnetic field. This, in turn, calls for the development of a special magnet power supply, based on Fourier synthesis.

Clearly, the simple system and mode of operation described above is quite inefficient. However, it is hoped that the results of this qualitative demonstration will encourage further investigation and development leading to efficient thermionic a.c. generation.

## SECTION VI - REFERENCES

1. A. Schock, J. Appl. Phys. 31, 1978 (1960).
2. A. Schock and C.L. Eisen, J. Appl. Phys. 33, 1 (1962).
3. A. Schock, J. Appl. Phys. 32, 1564 (1961).
4. C.L. Eisen and A. Schock, "Thermionic A.C. Generation," Am. Inst. Elec. Engrs., CP 62-1160 (1962).
5. V.C. Wilson, "Cesium Converter Studies," American Rocket Society, Conference Paper 1282-60.

PPL-TR-62-25

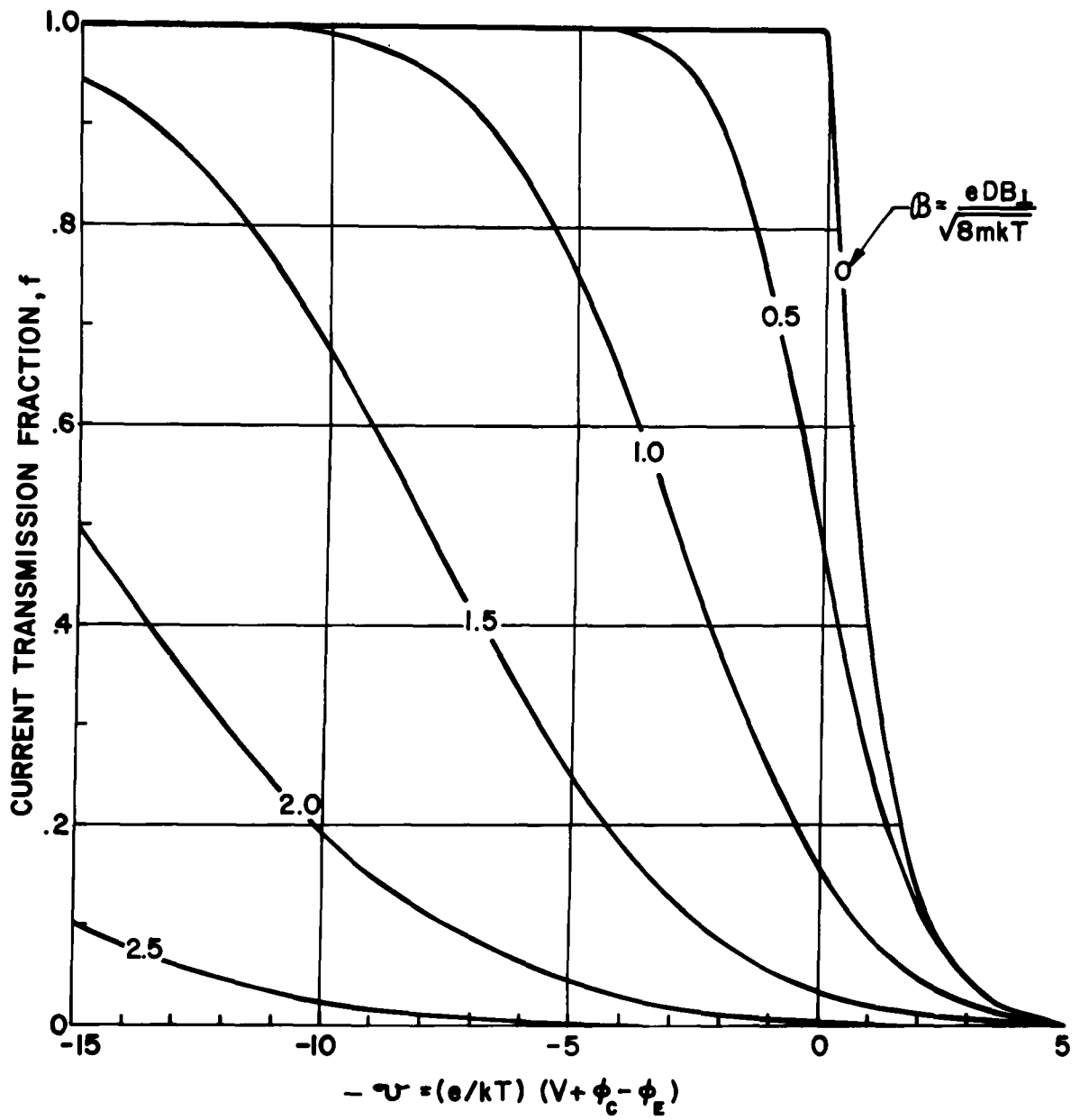


Figure 5. Theoretical Effect of Diode Voltage  $V$  and Transverse Magnetic Field  $B_{\perp}$  On Current Transmission

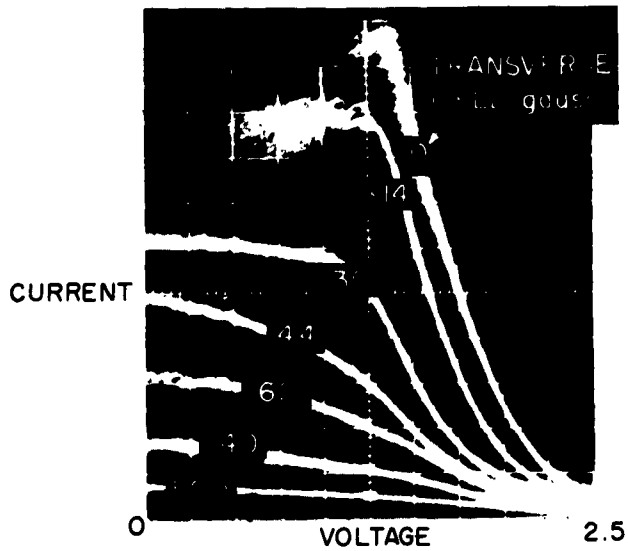


Figure 6. Transverse Field Effect in Low Pressure Diode ( $T_{CS} = 75^{\circ}\text{C}$ )

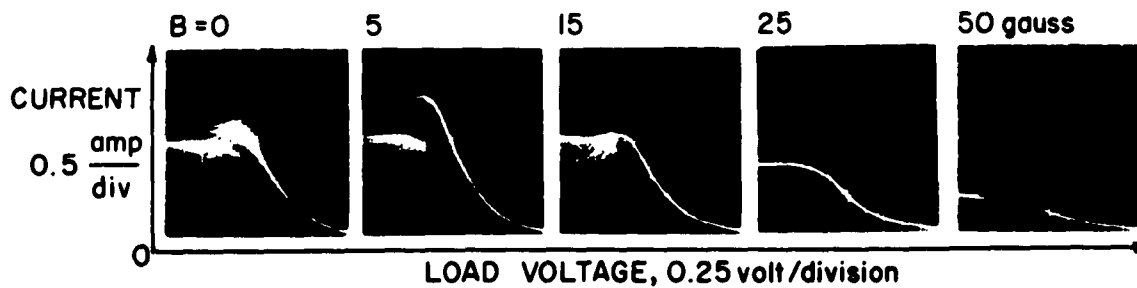


Figure 7. Effect of Transverse Fields on Oscillations ( $T_{CS} = 75^{\circ}\text{C}$ )

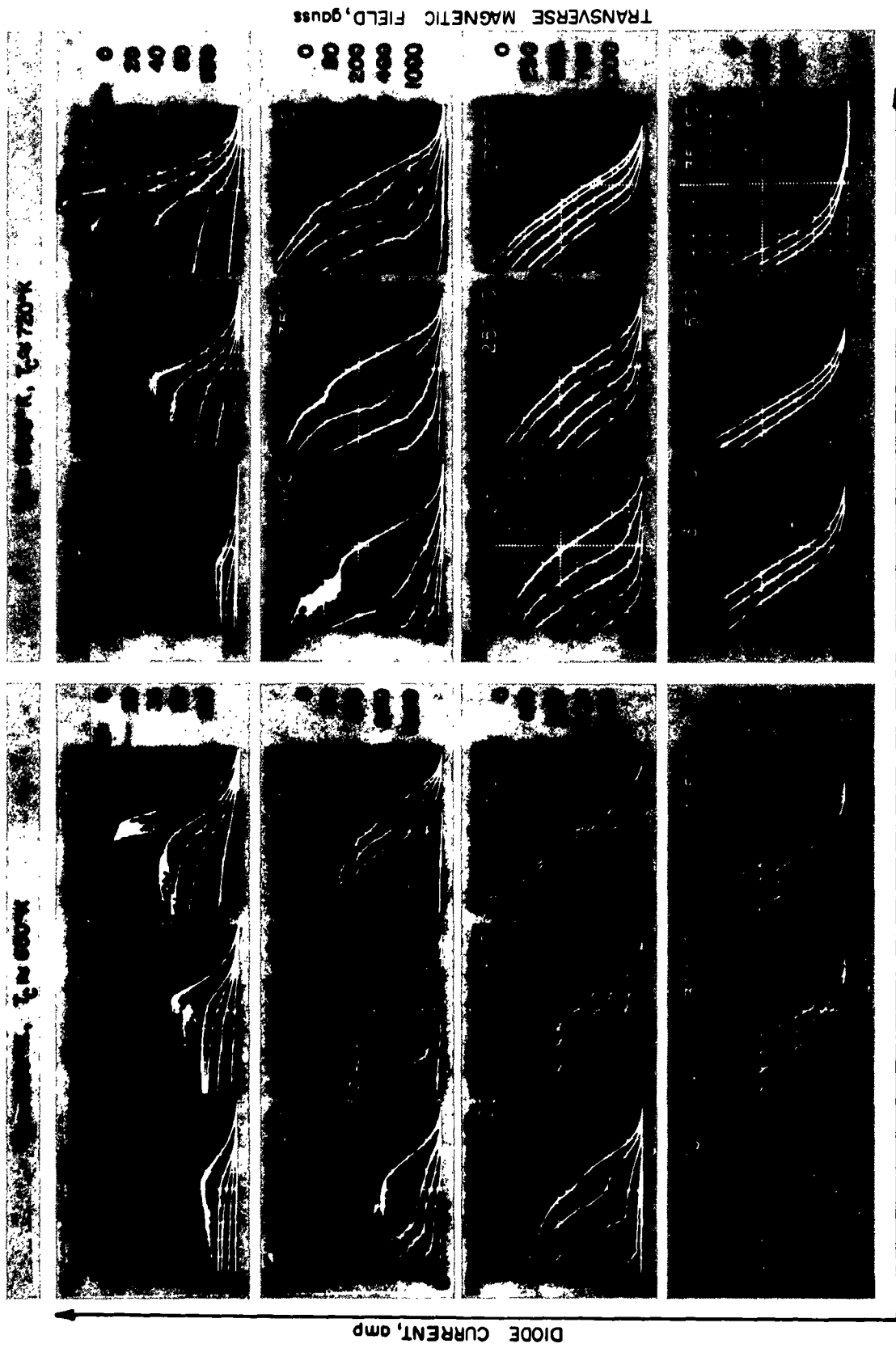


Figure 8. Transverse Field Effects on Current-Voltage Characteristics at Various Cesium Pressures

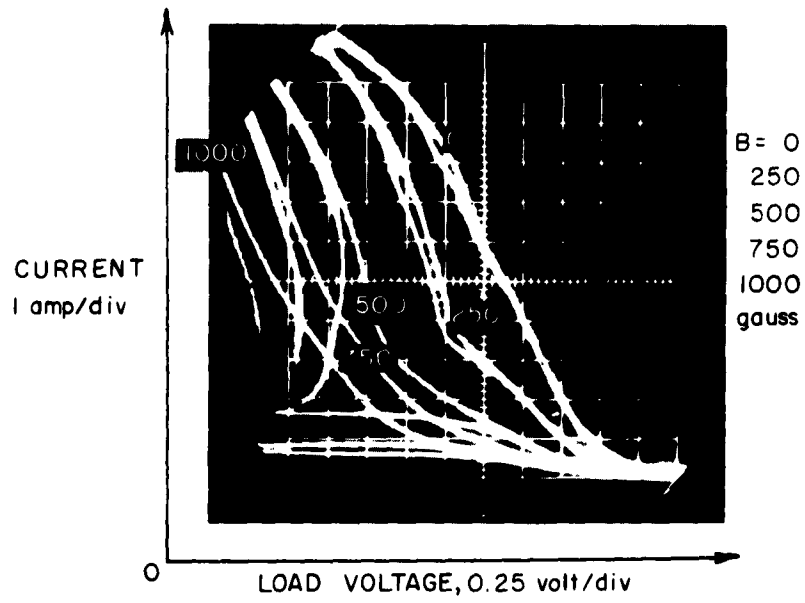


Figure 9. Ignited Diode Operation in Presence of Transverse Magnetic Fields ( $T_{CS} = 250^\circ\text{C}$ )

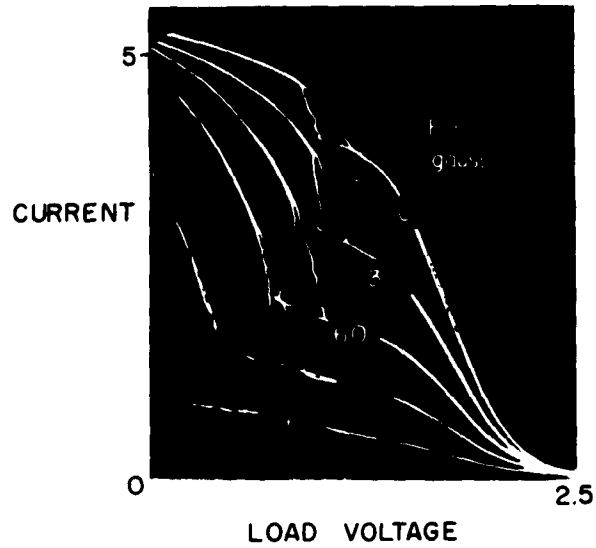


Figure 10. Effect of Transverse Fields on Ignition Voltage ( $T_{CS} = 150^\circ\text{C}$ )

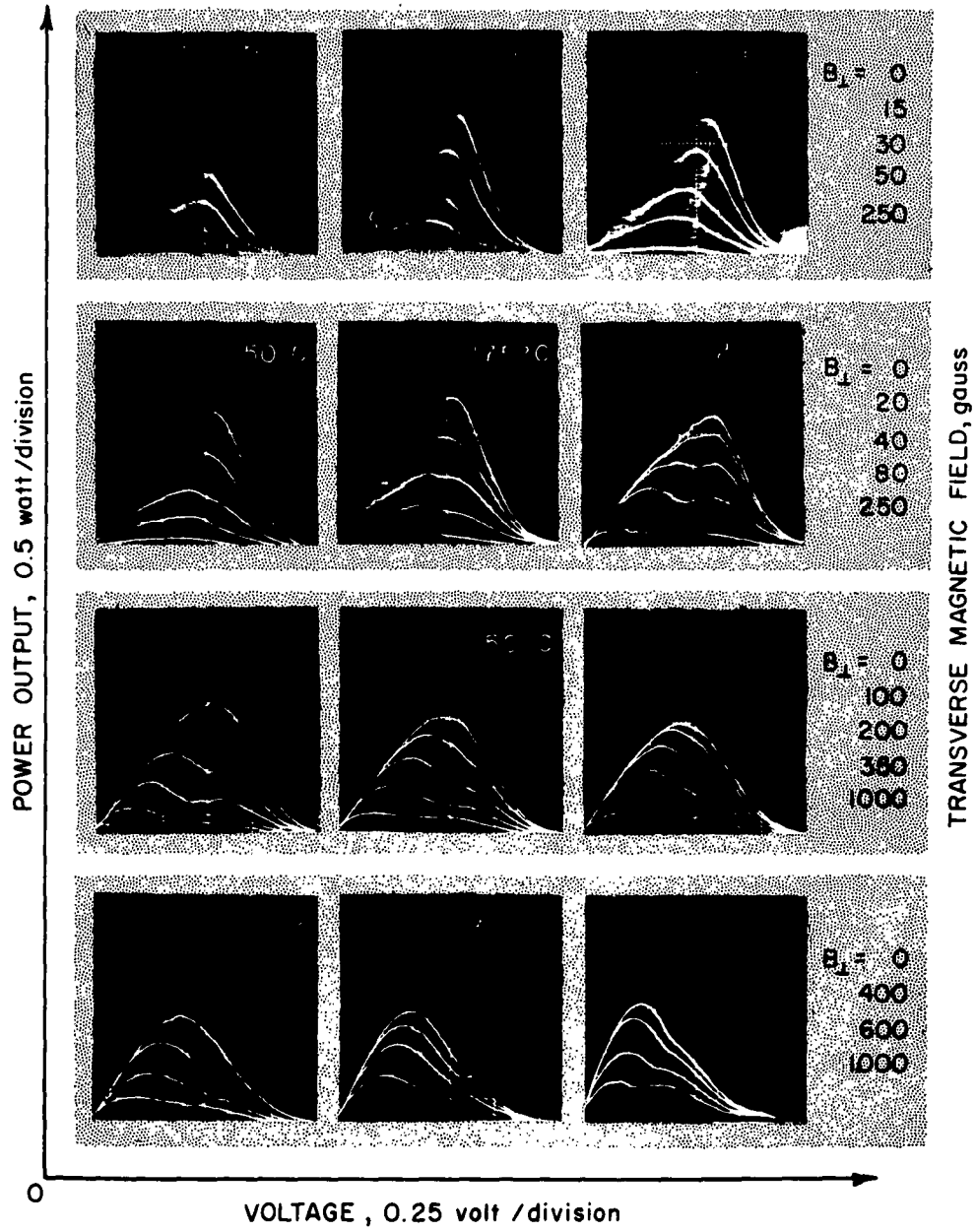


Figure 11. Transverse Field Effects on Power-Voltage Characteristics at Various Cesium Pressures ( $T_{\epsilon} \approx 1800^{\circ}\text{K}$ )

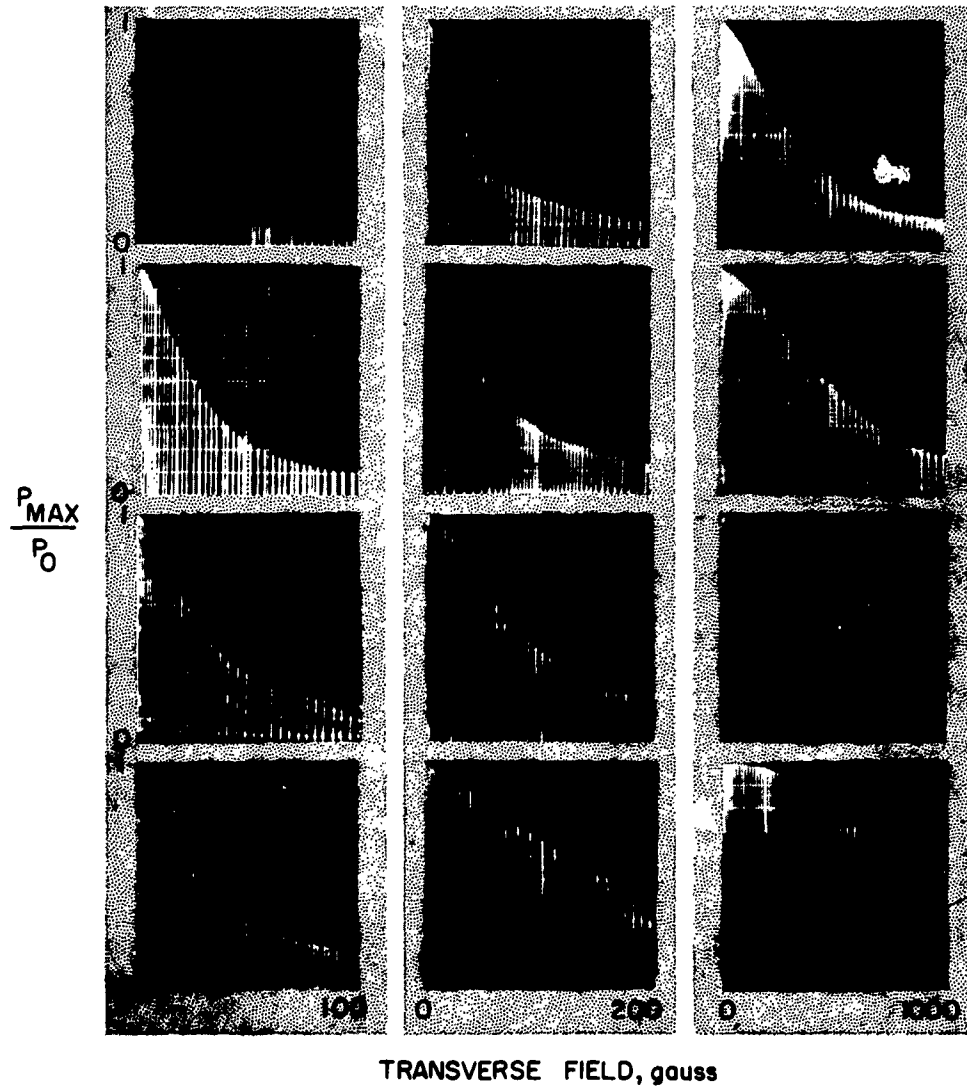


Figure 12. Effect of Transverse Fields on Maximum Power Output, at Various Cesium Pressures ( $T \approx 1800^\circ\text{K}$ )

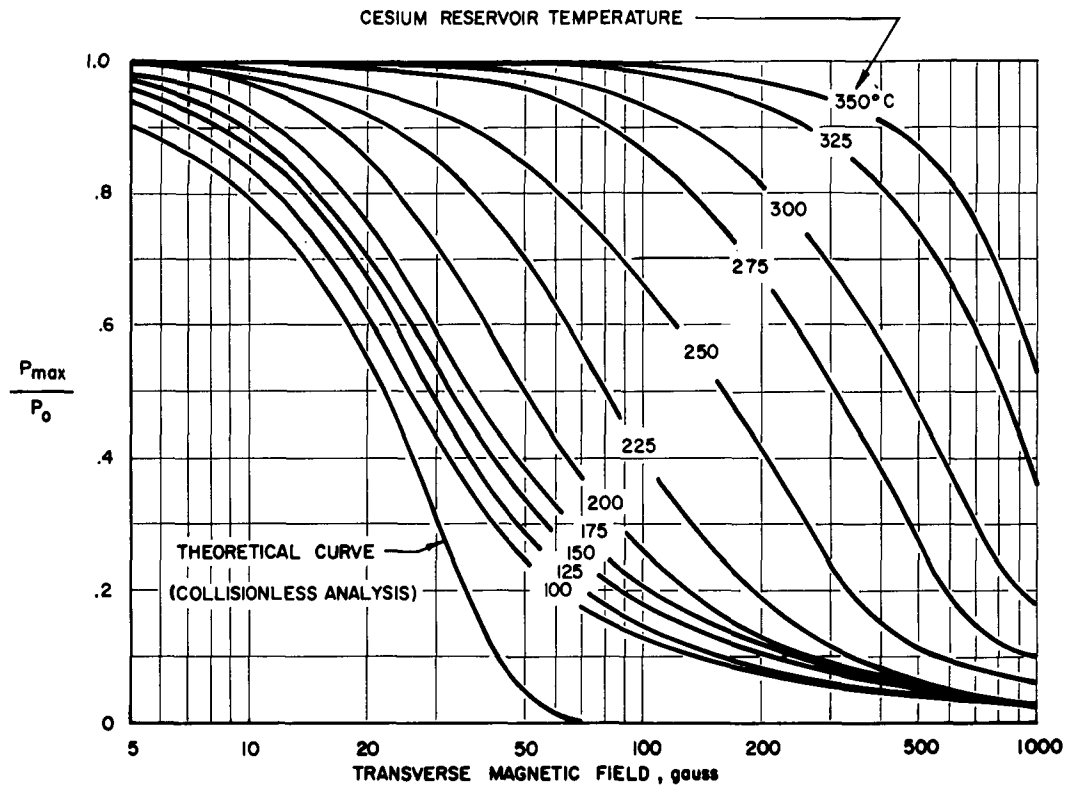


Figure 13. Comparison of Theoretical and Measured Magnetic Field Effects on Maximum Power Output ( $T_{\epsilon} \approx 1800K$ )

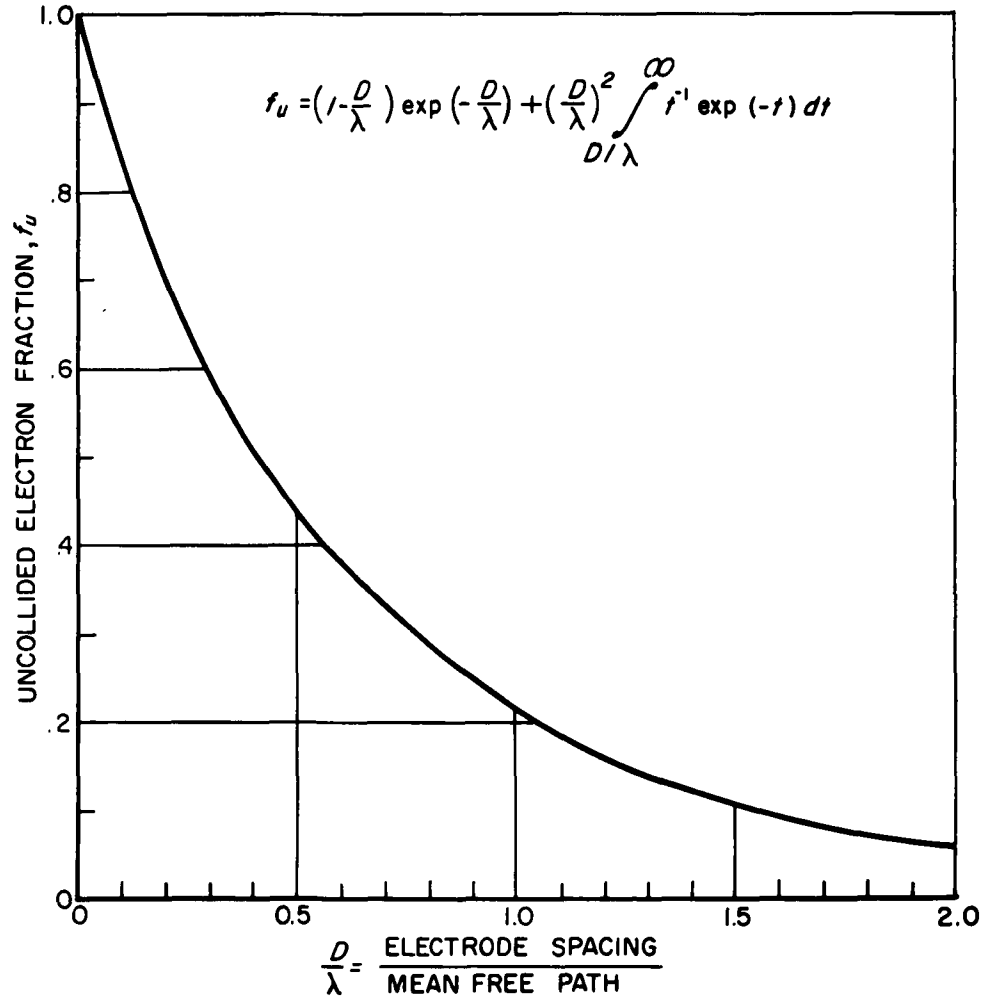


Figure 14. **Theoretical Fraction of Electrons Reaching Collector Without Suffering Collisions**

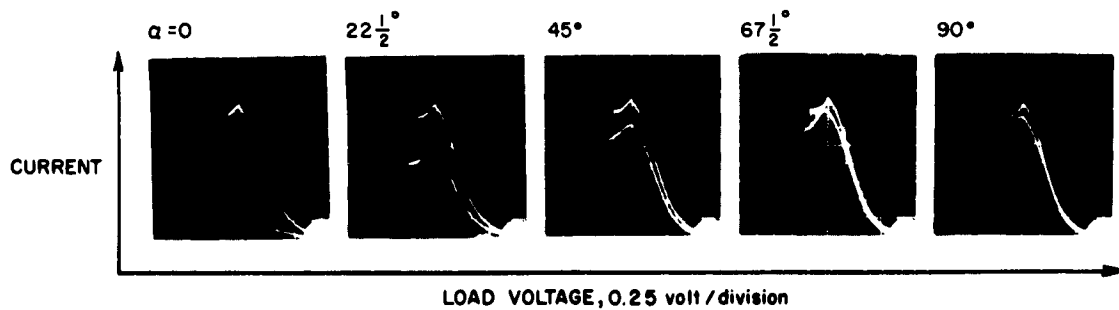


Figure 15. Effect of Strong Magnetic Field at Various Orientations  
(Top Curves,  $B = 0$ . Bottom Curves,  $B = 400$  Gauss)

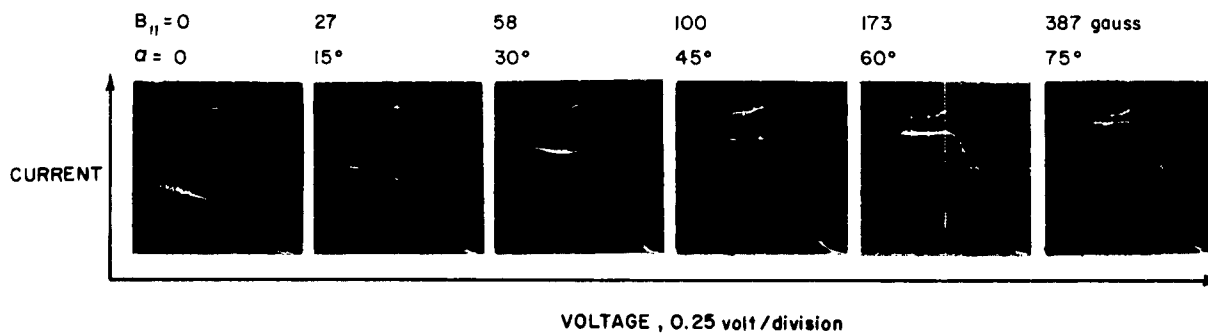


Figure 16. Effect of Various Longitudinal Fields  $B_{\parallel}$   
with Constant Transverse Field  $B_{\perp}$   
(Top Curves,  $B_{\parallel} = 0$ ; Bottom Curves,  $B_{\parallel} = 100$  gauss)

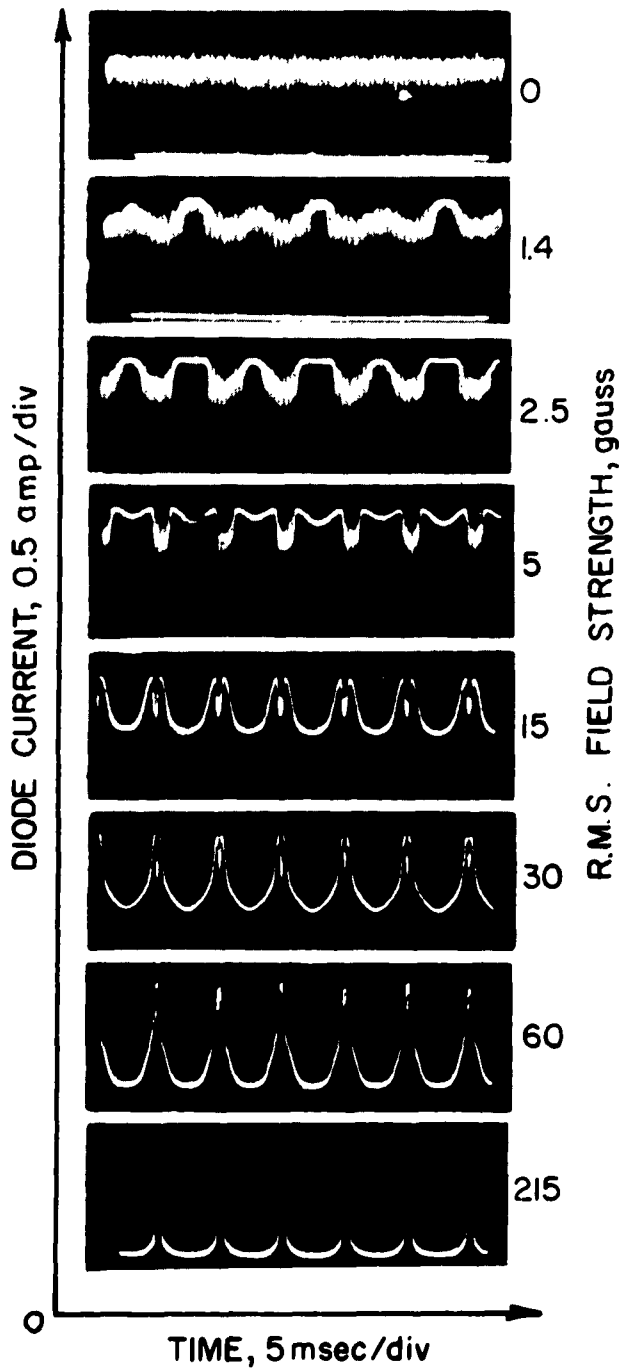


Figure 17. Effect of Sinusoidal Magnetic Fields On Oscillatory Diode  
 ( $T_{CS} = 75^{\circ}\text{C}$ )

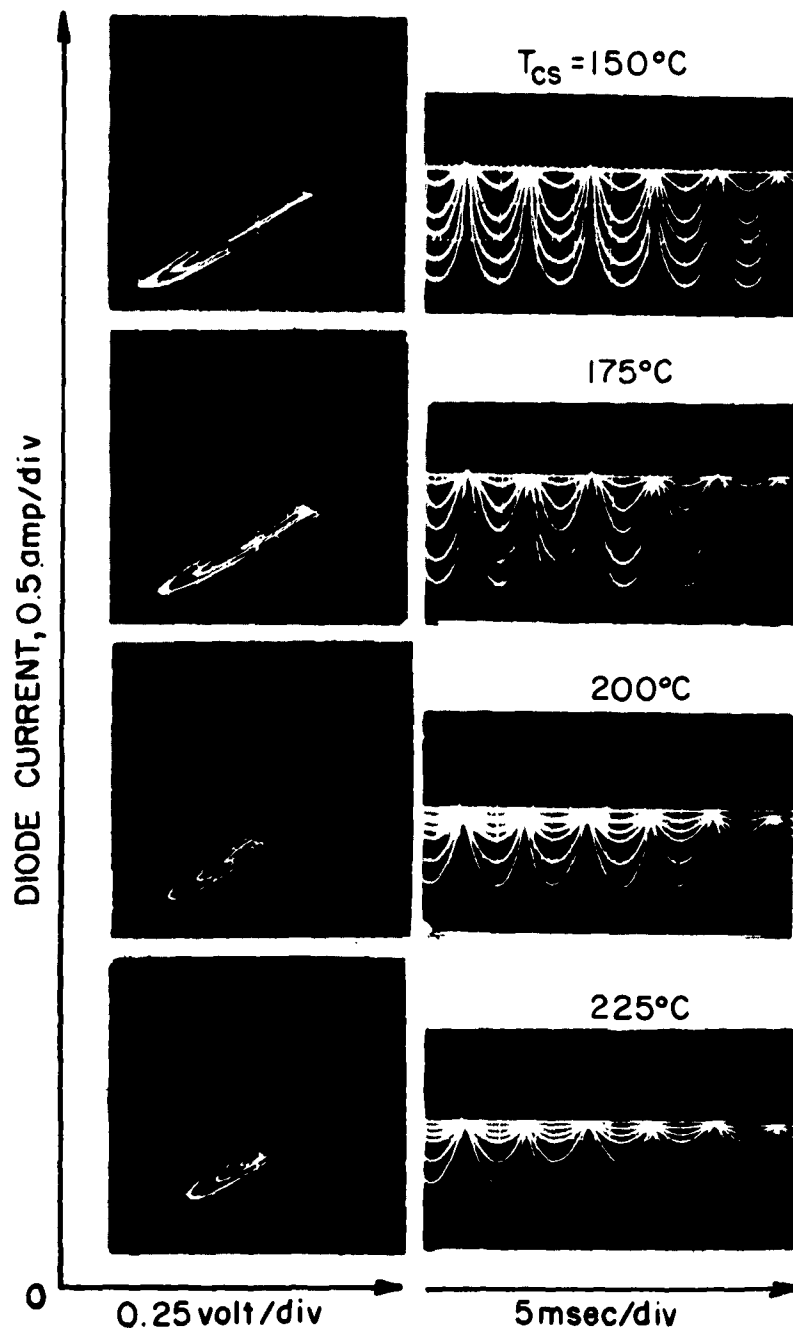


Figure 18. Effect of Sinudoidal Magnetic Fields on Thermionic Diodes at Various Cesium Pressures .  $B_{rms}$  (top to bottom) = 0, 20, 40, 60, 120, 215 Gauss

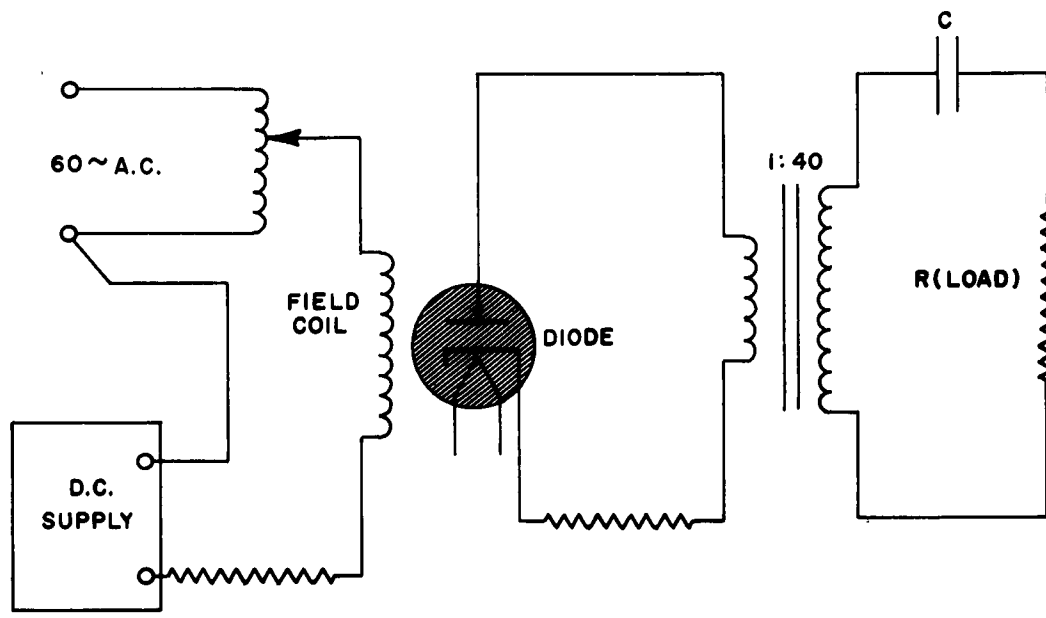


Figure 19. Circuit for Demonstrating A.C. Generation

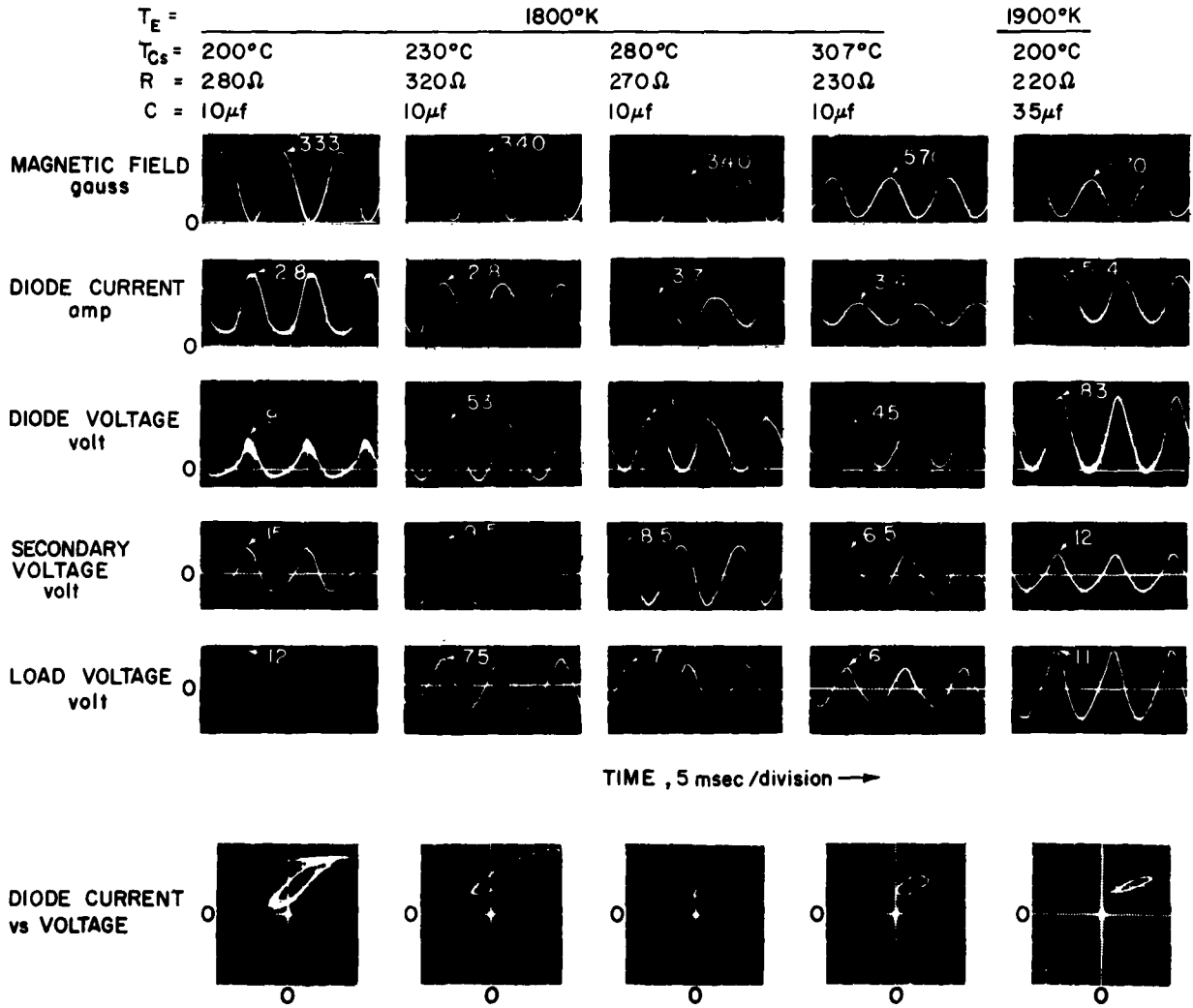


Figure 20. Typical Results of A. C. Demonstration

## APPENDIX A

## MASTER DISTRIBUTION LIST

## 099 - Energy Conversion

	<u>No. copies</u>
Office of Naval Research Power Branch (Code 429) Department of the Navy Washington 25, D. C.	4
Cognizant ONR Area Branch Office	1
U.S. Naval Research Laboratory Technical Information Division Washington 25, D. C.	6
U.S. Naval Research Laboratory Washington 25, D. C. Attn: Code 6430	1
Commanding Officer Office of Naval Research Branch Office Box 39 Navy #100 Fleet Post Office New York, N. Y.	2
Office of Technical Services Department of Commerce Washington 25, D. C.	1
Armed Services Technical Information Agency Arlington Hall Station Arlington 12, Virginia	10
National Aeronautics & Space Administration 1520 H Street, N. W. Washington 25, D. C. Attn: James J. Lynch	1
National Aeronautics & Space Administration Lewis Research Center 2100 Brookpark Road Cleveland 35, Ohio Attn: Frank Rom	1
	1
	1
Chief of Naval Operations (OP-07G) Department of the Navy Washington 25, D. C.	1

No. copies

Chief, Bureau of Ships Department of the Navy Washington 25, D. C. Attn: Code 342B Code 1500, LCDR J. H. Weber	1 1
Division of Reactor Development U.S. Atomic Energy Commission Washington 25, D. C. Attn: Auxiliary Power Branch Direct Conversion Branch	1 1
Aeronautical Systems Division ASRMFP-2 Wright Patterson Air Force Base Ohio	2
Air Force Cambridge Research Center (CRZAP) L. G. Hanscom Field Bedford, Massachusetts	1
Power Information Center University of Pennsylvania Moore School Building 200 South 33rd Street Philadelphia 4, Pennsylvania	1
Director of Special Projects (SP-001) Department of the Navy Washington 25, D. C.	10
Los Alamos Scientific Laboratory P.O. Box 1663 Los Alamos, New Mexico Attn: Dr. George M. Grover	1
Argonne National Laboratory 9700 South Cass Avenue Argonne, Illinois Attn: Aaron J. Ulrich	1
Director, Advanced Research Projects Agency The Pentagon Washington 25, D. C. Attn: Dr. John Huth	2
U.S. Army Signal R&D Laboratory Fort Monmouth, New Jersey Attn: Emil Kittil	1

No. copies

Mr. A. F. Underwood Manager, General Motors Research Labs. 12 Mile and Mound Road Warren, Michigan Attn: Dr. F. Jamerson	1
Atomics International P.O. Box 309 Canoga Park, California Attn: Dr. R. C. Allen	1
General Atomic P.O. Box 608 San Diego 12, California Attn: Dr. R. W. Pidd Dr. R. C. Howard	1 1
Republic Aviation Farmingdale Long Island, New York Attn: A. Schock	1
Allied Research Associates, Inc. 43 Leon Street Boston 15, Massachusetts Attn: Dr. P. Goodman	1
Ford Instrument Company 3110 Thomas Avenue Long Island City, N. Y. Attn: T. Jarvis	1
Armour Research Foundation 10 W. 35th Street Chicago 16, Illinois Attn: Dr. D. W. Levinson	1
Jet Propulsion Laboratory California Institute of Technology 4800 Oak Grove Drive Pasadena, California	1
RCA Laboratories David Sarnoff Research Center Princeton, New Jersey Attn: Dr. L. S. Negaard	1
The Martin Corporation Baltimore 3, Maryland Attn: Dr. M. Talaat	1

No. copies

Thermo Electron Engineering Corporation 85 First Avenue Waltham 54, Massachusetts Attn: Dr. George Hatsopoulos	1
Hughes Research Laboratories 3011 Malibu Canyon Road Malibu, California Attn: Dr. R. C. Knechtli	1
Thomson Ramo Wooldridge, Inc. 7209 Platt Avenue Cleveland 4, Ohio Attn: Wm. J. Leovic	1
General Electric Research Laboratory Schenectady, New York Attn: Dr. V. C. Wilson	1
Westinghouse Electric Company Research Laboratories Boulak Road, Churchilboro Pittsburgh, Pennsylvania Attn: Dr. Max Gavbuny	1
General Telephone & Electronics Labs., Inc. Bayside 60, New York Attn: R. Steinitz	1
The Marquardt Corporation ASTRO Division 16555 Saticoy Street Van Nuys, California Attn: A. N. Thomas	1
Texas Instruments, Inc. P.O. Box 5474 Dallas 22, Texas Attn: Dr. R. A. Chapman	1
University of Denver Colorado Seminary Denver Research Institute Denver 10, Colorado Attn: Dr. Charles B. Magee	1

RAC 1102  
(PPL-TR-62-25)

January 1963  
(43 pages, 18 illustrations)

Unclassified

Magnetic Field Effects In Thermionic Plasma Diodes

Experiments to determine the effect of transverse and longitudinal magnetic fields on thermionic current transmission are described. The results obtained are in qualitative agreement with theoretical predictions, and suggest the possibility of using magnetic modulation for a.c. generation.

Address inquiries to: Power Conversion Systems Divisions  
Republic Aviation Corporation  
Farmingdale, L. I., N. Y.

RAC 1102  
(PPL-TR-62-25)

January 1963  
(43 pages, 18 illustrations)

Unclassified

Magnetic Field Effects In Thermionic Plasma Diodes

Experiments to determine the effect of transverse and longitudinal magnetic fields on thermionic current transmission are described. The results obtained are in qualitative agreement with theoretical predictions, and suggest the possibility of using magnetic modulation for a.c. generation.

Address inquiries to: Power Conversion Systems Divisions  
Republic Aviation Corporation  
Farmingdale, L. I., N. Y.

RAC 1102  
(PPL-TR-62-25)

January 1963  
(43 pages, 18 illustrations)

Unclassified

Magnetic Field Effects In Thermionic Plasma Diodes

Experiments to determine the effect of transverse and longitudinal magnetic fields on thermionic current transmission are described. The results obtained are in qualitative agreement with theoretical predictions, and suggest the possibility of using magnetic modulation for a.c. generation.

Address inquiries to: Power Conversion Systems Divisions  
Republic Aviation Corporation  
Farmingdale, L. I., N. Y.

RAC 1102  
(PPL-TR-62-25)

January 1963  
(43 pages, 18 illustrations)

Unclassified

Magnetic Field Effects In Thermionic Plasma Diodes

Experiments to determine the effect of transverse and longitudinal magnetic fields on thermionic current transmission are described. The results obtained are in qualitative agreement with theoretical predictions, and suggest the possibility of using magnetic modulation for a.c. generation.

Address inquiries to: Power Conversion Systems Divisions  
Republic Aviation Corporation  
Farmingdale, L. I., N. Y.

Office of Naval Research, Washington 25, D. C.  
MAGNETIC FIELD EFFECTS IN THERMIONIC PLASMA  
DIODES. Final Technical Rpt, Jan 63, 43 p, incl. illus,  
5 refs. Distribution List is appended.

Unclassified Report

Experiments to determine the effect of transverse and longitudinal magnetic fields on the thermionic current transmission are described. The results obtained are in qualitative agreement with theoretical predictions, and suggest the possibility of using magnetic modulation for a. c. generation.

( over )

1. Direct energy conversion  
2. Thermionics  
I. Task NR 099-350  
II. Contract Nonr-3285(00)  
III. Republic Aviation Corporation

Farmingdale, L. I., N. Y.  
IV. A. Schock  
V. Secondary Rpt No RAC 1102 (PPL-TR-62-25)

Office of Naval Research, Washington 25, D. C.  
MAGNETIC FIELD EFFECTS IN THERMIONIC PLASMA  
DIODES. Final Technical Rpt, Jan 63, 43 p, incl. illus,  
5 refs. Distribution List is appended.

Unclassified Report

Experiments to determine the effect of transverse and longitudinal magnetic fields on the thermionic current transmission are described. The results obtained are in qualitative agreement with theoretical predictions, and suggest the possibility of using magnetic modulation for a. c. generation.

( over )

1. Direct energy conversion  
2. Thermionics  
I. Task NR 099-350  
II. Contract Nonr-3285(00)  
III. Republic Aviation Corporation

Farmingdale, L. I., N. Y.  
IV. A. Schock  
V. Secondary Rpt No RAC 1102 (PPL-TR-62-25)